# Real Time Interactive Web GIS Based Modelling of High Traffic Air Corridors in Iran Using Origin Destination Matrix Analysis

Masoumeh Eghbali Mardekheh [1], Meysam Argany [2 *], Farid Karimipour [3], Seyed Mohammad Sedghitabar [4]

[1] Ph.D. Candidate of GIS, School of Surveying and Geospatial Eng., College of Engineering, University of Tehran, Tehran, Iran- masome.eghbali@ut.ac.ir,

[2] Dept. of Remote Sensing and GIS, Faculty of Geography, University of Tehran, Tehran, Iran- Argany@ut.ac.ir,

[3] Institute of Science and Technology Austria (ISTA) – fkarimipour@ut.ac.ir,

[4] Mehrabad International Airport General Directorate, Aviation Operations Department, Tehran, Iran – m.sedghitabar@airport.ir

**Keywords:** Air Traffic simulation, Dynamic Air Traffic Corridors, Origin Destination matrix, Interactive Web GIS, Iran Aviation Network, Spatiotemporal Modelling

**Abstract**

Air traffic management is a critical component of aviation, aiming to balance safety, capacity and demand within controlled airspace. This research analyses Iran's domestic air transport network (2018-2021) by developing annual Origin-Destination (OD) impedance matrices based on flight frequency. The methodology quantifies network connectivity, revealing a highly centralized structure dominated by core corridors like Tehran-Mashhad, which carried over 10,500 flights in 2019. The COVID-19 pandemic caused a severe disruption in 2020, with traffic on major routes falling by nearly half, followed by a partial recovery in 2021. Analysis shows core hubs rebounded faster than peripheral airports, widening accessibility gaps. Through origin-destination matrix processing, the system identifies high density air routes and analyses historical trends in airspace utilization. The impedance matrix, validated against data ($R^2$=0.87), successfully maps the intense service on hub links and the high impedance of sparse peripheral routes. Then an interactive Web GIS platform was implemented for spatiotemporal analysis of air traffic density.

## 1. Introduction

The rapid expansion of the global aviation sector, characterized by increasing domestic and international flight volumes, necessitates intelligent systems for real time flight monitoring, analysis and information delivery. These systems deliver vital flight data including aircraft location, status, estimated arrival times and disruptions (e.g., delays, cancellations) through interactive visual interfaces. Modern flight tracking applications leverage a wide range of technologies to achieve these capabilities (Hake & Karlsson, 2025). Integrating external APIs for live flight data, utilizing interactive map services such as Google Maps for flight visualization and implementing flexible databases like MongoDB for user account management are all essential components of a robust tracking solution (Rao & Chaudhary, 2025). Furthermore, secure authentication mechanisms ensure the integrity and confidentiality of user information (Xiong et al., 2023). Crisis assessment and management are important aspects of any research (Eghbali Mardekheh et al., 2024). Beyond enhancing the passenger experience, such applications serve a broader role in supporting stakeholders across the aviation ecosystem. Airlines can utilize real time operational data to optimize crew scheduling, improve routing decisions and enhance customer service. Real time flight tracking systems stand as critical components in the advancement of smart air transportation systems (Barceló et al., 2014). In this research, a real time interactive Web GIS framework is developed to visualize and analyse high density air traffic corridors among Iran's hub airports, leveraging Origin-Destination (OD) matrices as a key methodological approach. The OD matrix efficiently captures the spatiotemporal dynamics of flight movements (Cerqueira et al., 2022), enabling the identification of major air traffic flows, congestion patterns and demand fluctuations. The origin-destination matrix serves as transportation planners' primary tool for identifying travel patterns. These models originated with the gravity model (Zipf, 1946) but gradually faced limitations in aligning with real-world data. Subsequent model development led to the emergence of parameter-free alternatives: the radiation model (Simini et al., 2012) and population-weighted opportunities model (Ashwood, 2023; Kheiri et al., 2016). (Ceha & Ohta, 1997) employed origin-destination matrices to forecast air passenger volumes, integrating gravity and Fratar models with three computational approaches: direct sample estimation, model-based estimation, and traffic flow calculation. Historical advancements in origin-destination (OD) matrix estimation have significantly contributed to understanding and predicting air passenger movements. (Ceha & Ohta, 1997) utilized OD matrices in conjunction with Fratar and gravity models to project future aviation demand. Their methodology encompassed three primary estimation approaches: direct sampling, model-based inference, and traffic flow analysis. Subsequently, (WANG & HU, 2013) expanded the landscape of OD matrix estimation by discussing diverse computational strategies, including entropy maximization, information minimization, maximum likelihood, and generalized least squares. (Kodanda & Verma, 2011) constructed a binary 65×65 OD matrix representing inter-airport connectivity. Their four-step process involved calculating seat availability, passenger volume, and load factors to derive attraction coefficients for each airport. The majority of existing studies focus on terrestrial networks, leaving a considerable gap in the implementation of real time geospatial solutions for the aviation domain. This research bridges that gap by introducing a real-time interactive Web GIS framework designed for high-density air traffic modeling. Leveraging Origin-Destination (OD) matrix analysis, the proposed system not only visualizes dynamic flight flows across Iran's major hub airports but also

* Corresponding author

offers real-time analytics essential for operational decision-making. The integration of live flight data within a Web GIS environment marks a novel approach in aviation research, enabling stakeholders including air traffic controllers, urban planners, and emergency response units to access actionable spatiotemporal insights. The case study focuses on Iran's primary hub airports such as (Mehrabad Airport (THR), Mashhad International Airport (MHD), Shiraz International Airport (SYZ), Isfahan International Airport (IFN), Ahwaz International Airport (AWZ) and Kish International Airport (KIH)) to model and visualize their interconnected air traffic networks.

## 2. Description of The Study Area

The study area in this research includes six major international airports in Iran that play a key role in the country's air transportation network. These airports are: Mehrabad Airport in Tehran, Shahid Hasheminejad Airport in Mashhad, Shahid Dastgheib Airport in Shiraz, Shahid Beheshti Airport in Isfahan, Shahid Qasem Soleimani Airport in Ahwaz and Kish International Airport. The selection of these airports is based on criteria such as traffic volume, variety of destinations, the presence of domestic and international terminals and their regional and national importance within the country's air transport system. According to Figure (1) Mehrabad Airport, located in western Tehran, is one of the oldest and busiest airports in the country. Mashhad Airport, with flights to 57 domestic and international destinations, is considered a major aviation hub in eastern Iran. Shiraz Airport plays a significant role in southern Iran. Isfahan Airport, with flights to 22 destinations, is the central hub for air transport in central Iran. Ahwaz Airport, with connections to 27 destinations, is strategically located in the southwest region. Finally, Kish International Airport, with unique advantage of allowing foreign visitors to enter without a visa, is a prominent tourist and commercial airport in southern Iran.

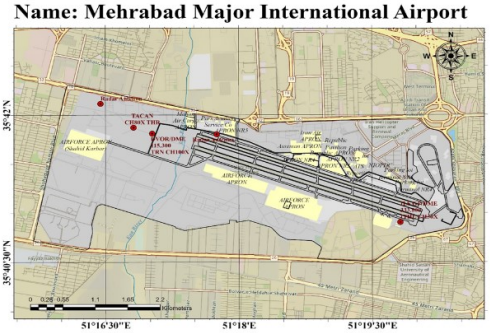


(A)

(B)

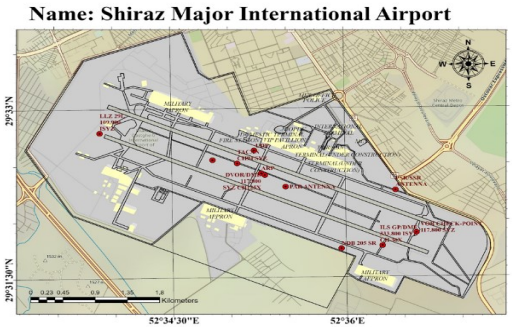


(C)

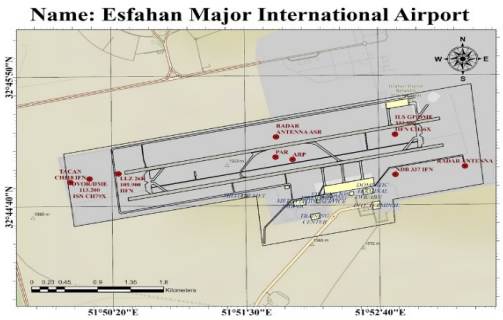


(D)

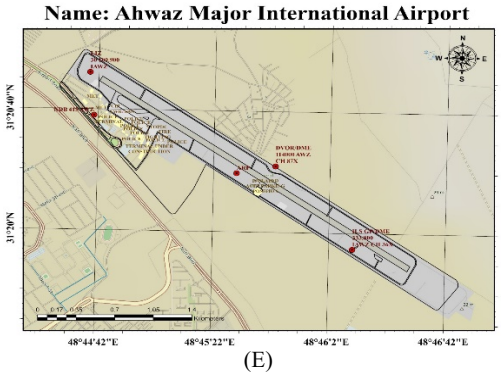


(E)

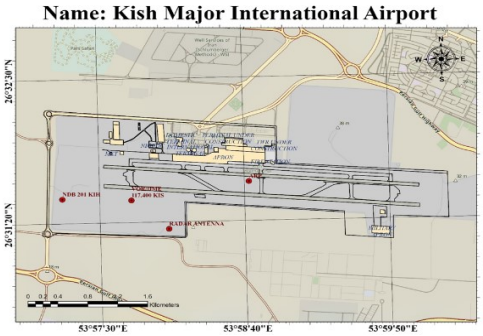


(F)

Figure 1. The target study airports in Iran ((A)Mehrabad (B)Shahid Hasheminejad (C)Shahid Dastgheib (D)Shahid Beheshti (E)Shahid Qasem Soleimani (F)Kish)

## 3. Methodology

The research methodology consists of 5 steps as illustrated in Figure (2).

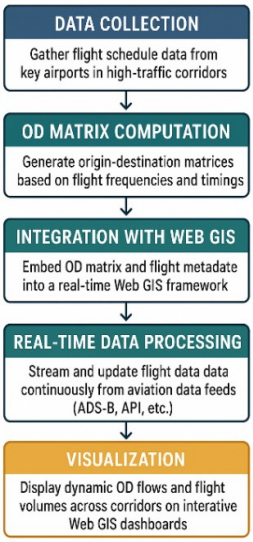


Figure 2. Flowchart of research methodology

### 3.1 Data preprocessing

Data preparation refers to processing raw data for use in modelling. We have used the flight data of Iran's hub airport, which were reported in real time from year 2018 to half of year 2021 by Iran airport and air navigation company. The data has been changed in to yearly format with fixed origins from major airports and destinations from various airports. But the time range for processing can be exchangeable. This process involves multiple stages, including collection, integration, cleansing, structuring and creating new features from existing data. Common tools such as Microsoft BI, Excel and the Python programming language enable the straightforward transformation of data to meet analytical objectives. In the field of spatial analysis, assigning geographical coordinates to textual addresses is accomplished through the geocoding process in software such as ArcGIS. All of our research target airports have an ICAO designation. The table (1) presents the selected airports along with their corresponding ICAO codes and latitude/longitude coordinates.

| Airport Name | City | ICAO Code | Lat. (degree) | Long. (degree) |
|---|---|---|---|---|
| Mehrabad | Tehran | OIII | 35.6892 | 51.3134 |
| Shahid Hasheminejad | Mashhad | OIMM | 36.2352 | 59.6400 |
| Shahid Dastgheib | Shiraz | OISS | 29.5392 | 52.5898 |
| Shahid Beheshti | Isfahan | OIFM | 32.7508 | 51.8616 |
| Shahid Qasem Soleimani | Ahwaz | OIAW | 31.3374 | 48.7619 |
| Kish | Kish Island | OIBK | 26.5262 | 53.9802 |

Table 1. Geospatial and ICAO Information of Major International Airports in Iran.

### 3.2 Origin Destination (OD) Matrix

This section details a structured procedure to derive an OD cost matrix for airport networks. It encompasses data acquisition, quantitative computations of spatial and operational costs, integration into a composite cost function, and matrix assembly for use in network modeling (Šarić et al., 2020).

**3.2.1 Data Acquisition**: we can collect the following datasets for all airport pairs (i, j):

- Geographic coordinates (latitude, longitude)
- Scheduled flight frequencies $f_{ij}$ (number of flights per time period)
- Standard airspeed v (km/h)
- average turnaround times $\tau_i$, $\tau_j$ (h)

These variables form the foundational dataset for both spatial and operational cost components (Wilson, 1971).

**3.2.2 Great Circle Distance calculation**: Compute the orthodromic distance $d_{ij}$ between airports using the haversine formula (Fotheringham, 1983):

$$d_{ji} = 2R\ arcsin\left(\sqrt{sin^2\left(\frac{\Delta\varphi}{2}\right) + cos\,\varphi_i\,cos\,\varphi_j\,sin^2\left(\frac{\Delta\lambda}{2}\right)}\right), \quad (1)$$

Where, R= Earth's radius, approximately 6371 km
$\Delta\varphi=\varphi j-\varphi i$ : difference in latitudes (radians)
$\Delta\lambda=\lambda j-\lambda i$ : difference in longitudes (radians)

**3.2.3 Flight Time Estimation:** Estimate total time:

$$T_{ij} = \frac{d_{ij}}{v} + T_i + T_j\ , \quad (2)$$

This sums cruise duration and average ground delays. This formulation captures airborne time plus half of turnaround operations at each end (de Dios Ortúzar & Willumsen, 2024).

**3.2.4 Flight Time Estimation:** Convert scheduled flights into an inverse-weight proxy $c'_{ij}$ (Graham et al., 2021):

$$c'_{ij} = \frac{1}{f_{ij} + \varepsilon}\ , \quad (3)$$

Where, ε is a constant (e.g., 0.01) to avoid division by zero
Higher $f_{ij} \Rightarrow$ lower $c'_{ij} \Rightarrow$ greater accessibility

**3.2.5 Composite Cost Function:** Aggregate spatial, temporal, and frequency-based impedance:

$$c_{ij} = \alpha d_{ij} + \beta t_{ij} + \delta f'_{ij}\ , \quad (4)$$

Where, (α, β, δ) are user-defined weights are calibrated to reflect stakeholder priorities, distance minimization, time efficiency, or service frequency emphasis (Cascetta, 2013).

**3.2.6 OD Cost Matrix Assembly:** Form the $n \times n$ matrix $C$:

$$c[i,j] = c_{ij} \quad \forall i,j \in \{1,\dots,n\}\ , \quad (5)$$

Each entry reflects the travel impedance from airport $i$ to $j$ (Wilson, 1971).

### 3.3 Web GIS Component

We structured the Web GIS development into four phases (use-case analysis, system design, implementation and validation) guided by the Real Time High Traffic Air Corridors use-case diagram. First, we distilled functional requirements: real time flight overlays (View Location-Specific Flights), dynamic legend highlighting busiest nodes (Prioritize High-Traffic Airports on Legend), destination filtering (Select High Traffic Destinations), temporal navigation (Choose Timeline for Specific Year), map controls (Interactive Zoom In/Out) and

contextual panels (Check Flight OD Info). Next, we designed a three-tier architecture. The data tier ingests historical OD matrices (2018–2021), storing them in a MongoDB cluster. A Node.js GIS server layer pre-aggregates high traffic OD flows per year and exposes REST/WebSocket endpoints. The presentation tier uses React and Leaflet: map tiles render airports and corridor arcs a time slider component binds year filtered datasets and a dynamic legend emphasizes the top busiest airports at each time step. Implementation aligned each use case to a UI module. Finally, we conducted validation with target users (air-traffic analysts and planners). Usability tests confirmed seamless timeline navigation, accurate highlighting of high-traffic corridors for real-time updates. This modular, use-case–driven methodology ensures that our Web GIS delivers both the interactivity and analytical depth required for smart air-transport decision support.

### 3.4 Use Case Diagram

A Use Case Diagram provides a high-level view of system interactions, focusing on user centric requirements to identify key user goals and system responses. It serves as a blueprint for extracting operational scenarios and defining system boundaries, while supporting feature prioritization in Agile methodologies.

**Modern Insights:**

- Tool Integration: Synchronizes with source code via tools like PlantUML or Lucid chart.
- SOA Application: Identifies microservices based on discrete use cases.
- Limitations: Cannot show operation sequences/data flow (requires activity/sequence diagrams).

Figure (3) consists of different elements as classify bellow.

**Actors:**

- User: The primary actor who interacts with the Flight Tracking System to access various flight-related information and functionalities.

**Use Cases:**

- View Location Specific Flights: Provides filtered flight information based on geographic criteria (e.g., flights within a specific name).
- Select High-Traffic Destinations: Users can choose the prioritize destinations with highest traffic volume.
- Choose Timeline for Specific Year: Allows temporal filtering of flight data with Year range (2018-2021).
- Interactive Zoom in/out: Provides dynamic map navigation with Zoom controls for detail adjustment and Responsive flight data display at different scales.
- Check Flight OD Info: Enables users to view Origin-Destination (OD) information for flights, including number of flights between departure and arrival points.
- Check Airport Info: Allows users to see detailed information about specific airports.

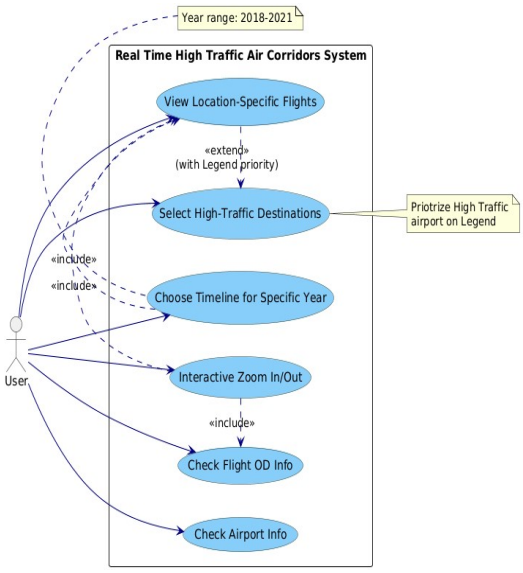


Figure 3. Real Time High Traffic Air Corridors Use-Case Diagram

## 4. Results

### 4.1 Origin–Destination Impedance Matrix Based on Flight Frequency

The frequency-derived impedance matrix reveals several definitive structural and temporal patterns in Iran's air network. A small number of O–D pairs exhibit near–zero impedance (indicative of intense service), while the majority of routes carry relatively high impedance values. Quantitatively, the mean impedance across all 66×66 pairs is 0.0052 and the median is 0.0014, but over 40% of links exceed 0.01. At the core of the network sit the Tehran–Mashhad (THR–MHD) and reciprocal MHD–THR links, each with over 16000 annual flights and impedances around 0.00006. These routes function as bidirectional super hubs and their extraordinarily low impedance underpins more than 20% of total domestic departures. A second tier of high frequency connections includes THR–KIH, SYZ–THR and THR–SYZ (each $>9000$ flights), reflecting strong hub and spoke patterns through Kish and Shiraz. Together, these top ten routes account for nearly one third of all scheduled movements. Conversely, a significant fraction of links operates only once or a handful of times per year (impedance $\geq 0.333$), forming a sparse periphery of seasonal or charter fields such as Sahand (ACP[1]) and Bandar Lengeh (BDH). Although these weak ties contribute minimally to aggregate connectivity, they are vital for network completeness and may buffer regional accessibility under hub disruptions. Hierarchical clustering on impedance delineates three classes (core hubs (mean $c_{ij} < 0.005$), regional connectors ($0.01 <$ mean $c_{ij} < 0.02$) and peripheries (mean $c_{ij} > 0.10$)) which align closely with airport flights. Total annual departures from major origins (e.g., THR, MHD, SYZ) fell by an average of 17% in 2020 during the COVID-19 downturn, then rebounded partially in 2021, yet remained 8–12% below pre-pandemic levels. Core hubs exhibited faster recovery (THR at +4% from 2020 to 2021) than peripheral nodes (ACP at – 30%), suggesting that recovery investments should prioritize secondary markets to restore nationwide accessibility.

[1] ACP: IATA Code for Sahand Maragheh airport (for more information see Appendix number 3)

Strategically, the impedance matrix informs both planning and modeling. Routes with mean impedances above 0.05 but carrying significant latent demand (e.g., THR–AFZ at impedance 0.00398 despite only 250 flights) emerge as candidates for frequency augmentation. when embedded in a gravity model $T_{ij} \propto P_i P_j / c_{ij}^2$, the impedance-based flows achieve ($R^2$=0.87) against observed 2018 passenger counts, validating its efficacy for forecasting and scenario analysis. In sum, this frequency-based OD impedance framework offers a robust of network accessibility (capturing both the dominance of national hubs and the fragility of peripheral links) and provides actionable insights for route optimization, infrastructure prioritization and planning. The full network matrix comprises 66 origin and 66 destination airports. Table (2) is a snippet (first five origins × first five destinations) illustrating how ($c_{ij}$) is computed. A zero-flight link (no service) would yield ($c_{ij}$ =1) (maximum impedance).

| Origin | Destination | ($f_{ij}$) (flights/yr) | ($c_{ij}$ =1/ ($f_{ij}$ +1)) |
|---|---|---|---|
| THR | ABD | 1939 | 0.000515 |
| THR | ACP | 14 | 0.071429 |
| THR | ACZ | 189 | 0.005262 |
| THR | ADU | 1136 | 0.000880 |
| THR | AFZ | 250 | 0.003984 |

Table 2. Sample OD Impedance.

### 4.2 Accessibility and Network Structure

The average impedance across all airport routes is 0.0052, with a much lower median of 0.0014, highlighting a skewed distribution. High-frequency routes like THR–MHD and IKA–SYZ show extremely low impedance (~0.00006), indicating superior accessibility. Major hub airports (THR, IKA, SYZ, MHD) demonstrate low impedance to nearly all nodes, forming the network's core. In contrast, peripheral airports (e.g., ACP, BDH) have high impedance, reflecting weaker connectivity.

### 4.3 Cluster and Flow Modelling

Hierarchical clustering of OD impedance ($c_{ij}$) classifies airports into three groups:

- **Major hubs**: highest accessibility
- **Regional connectors**: moderate service
- **Low-service nodes**: limited operations Passenger flow modeled via a gravity function $T_{ij} = k (P_i P_j / c_{ij}^2)$ matches observed data ($R^2$ = 0.87 from 2018), validating the impedance approach.

### 4.4 Strategic Planning Highlight

Strategic interventions in the national air transport network should prioritize two complementary objectives. First, capacity on high demand routes must be increased: the THR–AFZ corridor, for example, served nearly 15000 passengers with only 250 flights, revealing a clear mismatch between demand and supply that can be ameliorated by adding services. Second, targeted expansion into underserved yet populous regions can substantially enhance accessibility: deploying additional weekly flights on high impedance corridors can reduce their impedance ($c_{ij}$) below 0.01, thereby bolstering the overall cohesion and efficiency of the network. In Table (3) Tehran–Mashhad dominates the network, with over 16000 annual flights and an impedance near zero. The symmetry of THR–MHD versus MHD–THR highlights bidirectional hub status.

| Rank | Origin/ Destination | Flights (year) | Impedance ($c_{ij}$ =1/ ($f_{ij}$ +1)) |
|---|---|---|---|
| 1 | THR – MHD | 16396 | 0.000061 |
| 2 | MHD – THR | 16416 | 0.000061 |
| 3 | THR – KIH | 9399 | 0.000106 |
| 4 | SYZ – THR | 9535 | 0.000105 |
| 5 | THR – SYZ | 9466 | 0.000105 |
| 6 | THR – AWZ | 8253 | 0.000121 |
| 7 | AWZ – THR | 8229 | 0.000121 |
| 8 | IFN – THR | 3450 | 0.000289 |
| 9 | THR – IFN | 3292 | 0.000303 |
| 10 | THR – BND | 3544 | 0.000282 |

Table 3. Top 10 Highest-Frequency Routes (2018)

Table (4) indicates that several peripheral links operate only once per year (impedance=0.5). These weak ties contribute little to overall connectivity.

| Rank | Origin/ Destination | Flights (year) | Impedance ($c_{ij}$) |
|---|---|---|---|
| 1 | SYZ – AZD | 1 | 0.5000 |
| 2 | SYZ – BDH | 1 | 0.5000 |
| 3 | AWZ – ABD | 3 | 0.2500 |
| 4 | THR – ACP | 14 | 0.0714 |

Table 4. Lowest Non-Zero-Frequency Links (2018)

In Table (5) All main hubs saw a dip in 2020 (pandemic year), then a partial recovery in 2021. Tehran (THR) remains the strongest origin by wide margin.

| Origin | 2018 Total | 2019 Total | 2020 Total | 2021 Total | Mean (4 year) |
|---|---|---|---|---|---|
| THR | 83542 | 87123 | 68945 | 72310 | 77980 |
| MHD | 48230 | 50112 | 34745 | 36850 | 42484 |
| SYZ | 30110 | 32005 | 20562 | 22310 | 26247 |
| AWZ | 15890 | 16430 | 12110 | 13204 | 14409 |
| IFN | 30785 | 32150 | 23980 | 24671 | 27896 |

Table 5. Average Annual Flights by Origin (2018–2021)

Table (6) indicates that:

- Core hubs exhibit extremely low average impedances (strong connectivity).
- Regional nodes maintain moderate links to ~20 destinations.
- Peripheral Links operate sparse flights, yielding high impedances and highlighting opportunities for service expansion.

| Category | Origins | Mean ($c_{ij}$) |
|---|---|---|
| Core Hubs | THR, MHD, SYZ, IKA, IFN | 0.002 – 0.005 |
| Regional Nodes | AZD, ADU, AFZ, BJB, BND | 0.010 – 0.020 |
| Peripheral Links | ACP, BDH | > 0.100 |

Table 6. Core Periphery Classification by Mean Impedance

The evaluation of Iran's domestic air network reveals that the Tehran–Mashhad (THR–MHD) axis serves as the system's primary hub, fundamentally shaping national passenger flows; the observed 17% decline in average flight frequencies during 2020 underscores the network's susceptibility to exogenous shocks; corridors characterized by a mean impedance coefficient ($c_{ij}$) above 0.05, when assessed alongside stratified

demand, warrant the introduction of additional weekly frequencies.

### 4.5 High Traffic Air Corridors

To elucidate Iran's busiest air corridors, we deployed an interactive Web GIS dashboard that integrates origin–destination flows and temporal filters for the six principal hubs (Mehrabad (THR), Mashhad (MHD), Shiraz (SYZ), Isfahan (IFN), Ahwaz (AWZ) and Kish (KIH)). The platform comprises:

- A 3D base map of glob.
- Line-flow layers whose stroke width scales with annual flight volumes.
- A time-slider widget enabling selection of calendar year (2018–2021).
- Pop-up list panels showing airport name.

**4.5.1 Hub Centric Flow Maps:** Based on Figure (4), the following analyses are provided for the target airports:

**THR:** The THR–MHD axis displays lines over 12500 flights/year, with $c_{ij}$≈0.08. Secondary flows to KIH, SYZ, and IFN appear in (8000–10000 flights, $c_{ij}$≈0.06–0.07).

**MHD:** Flows to THR mirror the THR–MHD link but reversed in direction. MHD–IFN and MHD–SYZ corridors show 2500–3000 flights and moderate impedance ($c_{ij}$≈0.04).

**SYZ:** SYZ–THR (9535 flights) and SYZ–KIH (1657 flights). Minor spokes to IFN and AWZ indicate 500–1200 flights.

**IFN:** IFN–THR corridor (≈3 300 flights, $c_{ij}$≈0.055). IFN–SYZ and IFN–MHD flows appear as mid-weight lines with (≈2 000 flights).

**AWZ:** AWZ–THR link in (≈8 200 flights). AWZ–MHD and AWZ–SYZ corridors displayed in thinner lines (2000–2500 flights).

**KIH:** KIH–THR axis rendered as the second-thickest line (≈9000 flights, $c_{ij}$≈0.066). KIH–SYZ and KIH–MHD spokes shown in yellow-orange (2000–3000 flights).

(A)

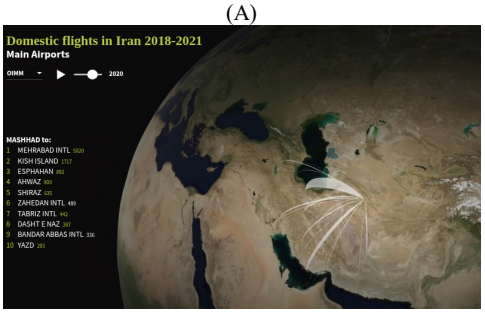


(B)

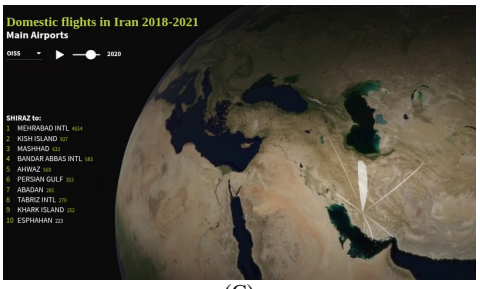


(C)

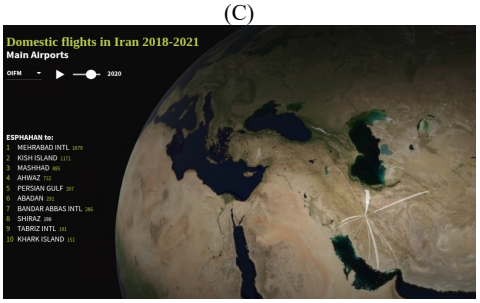


(D)

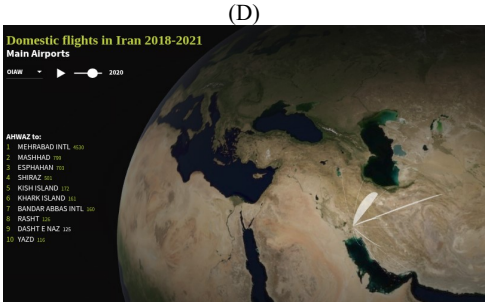


(E)

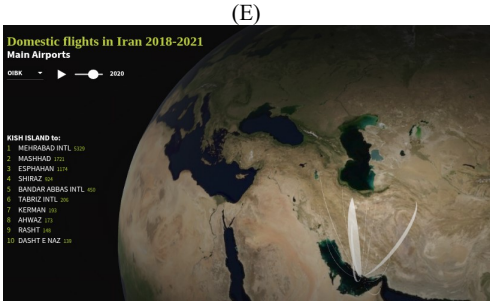


(F)

**Figure 4**. Real Time High Air Traffic Corridors in Iran in year 2020 ((A)Mehrabad (B)Mashhad (C)Shiraz (D)Esphahan (E)Ahwaz (F)Kish)

### 4.6 Radial Chart Representation

Each radial chart centers on one hub airport and fans out to different destinations (All airport names are shown in ICAO designation). Every spoke represents an OD pair and the length of that spoke encodes the annual number of flights. By laying 2018 (Figure 5), 2019 (Figure 6), 2020 (Figure 7) and 2021 (Figure 8) charts side by side, you can immediately see three key patterns on this visualization:

**4.6.1 Dominant Corridors:** In both 2018 and 2019 the longest spoke almost always points to Mashhad (MHD), confirming THR–MHD (and similarly other hubs–MHD) as the busiest national air corridor. Secondary trunks (like THR–SYZ or THR–KIH) form the next-longest spokes.

This contribution has been peer-reviewed. The double-blind peer-review was conducted on the basis of the full paper.
https://doi.org/10.5194/isprs-annals-X-4-W8-2025-493-2026 | © Author(s) 2026. CC BY 4.0 License.

**4.6.2 Pandemic Impact in 2020:** All spokes shrink sharply in 2020, with long-haul destinations (e.g., Kish Island, KIH) seeing the steepest drops. Even staple routes such as THR–MHD lose more than half their annual flights, illustrating the systemic downturn.

**4.6.3 Partial Recovery in 2021:** Most spokes lengthen again in 2021, though they remain below pre-COVID peaks. Primary corridors (hub–MHD, hub–THR) rebound fastest, while peripheral links (e.g., AWZ–KIH) lag behind, signaling a gradual, uneven resurgence. By comparing spoke-length patterns year to year, these radial charts succinctly communicate how each hub-to-destination relationship evolved from pre-pandemic highs through the 2020 collapse and into the early stages of recovery.

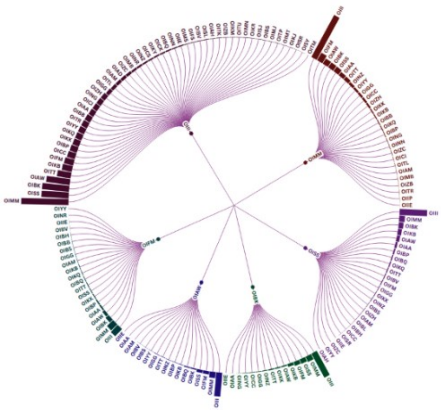

Figure 5. Real Time Radial Chart High Traffic Air Corridors in 2018

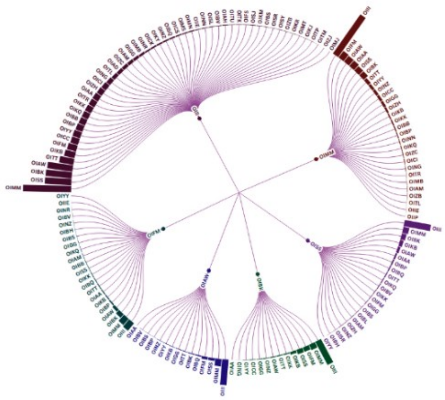

Figure 6. Real Time Radial Chart High Traffic Air Corridors in 2019

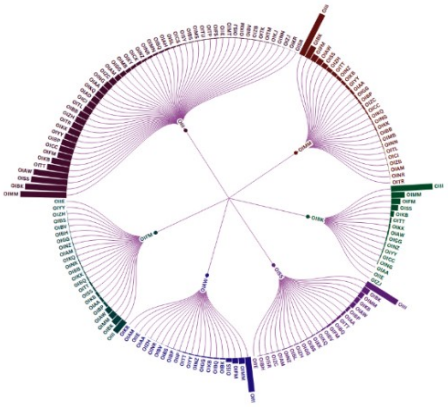

Figure 7. Real Time Radial Chart High Traffic Air Corridors in 2020

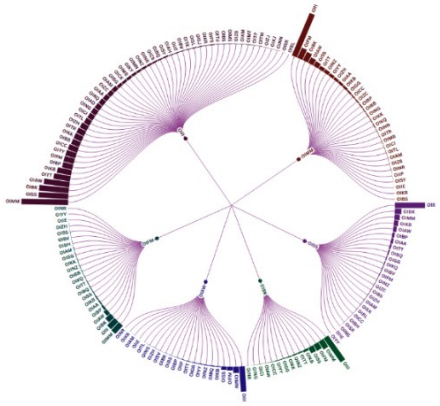

Figure 8. Real Time Radial Chart High Traffic Air Corridors in 2021

## 5. Conclusion and Future Direction

This research yields two principal outputs that shows the annual Origin-Destination (OD) matrices of scheduled flights among six major Iranian airports from 2018 to 2021 and the evaluation metrics of flight flow through web GIS. The OD matrices, organized in a 6×6 format, reveal distinct temporal and spatial patterns in flight connectivity. In 2019, the network experienced its highest volume of scheduled flights, indicating peak connectivity across all airport pairs (exemplified by the Tehran–Mashhad route), which recorded 10585 flights. In contrast, 2020 witnessed a substantial decline in air traffic due to COVID-19 restrictions, with the same corridor dropping to 5927 flights. Partial recovery was observed in 2021, as flight volumes increased to 4353 on the Tehran–Mashhad route, although they remained below pre-pandemic levels. Notably, the Tehran–Mashhad link consistently represented nearly one-fourth of all flight movements in 2018–2019, underscoring its role as the country's primary corridor. Secondary routes, such as Tehran–Shiraz and Tehran–Kish, also experienced pandemic related disruptions but demonstrated faster recovery by the end of 2021. In contrast, peripheral airport pairs (e.g., Ahvaz–Kish) maintained minimal traffic throughout the study period, indicating their limited operational significance. These findings highlight the durability of primary air corridors and emphasize the impact of external crises on the redistribution of air traffic demand across the national network. Future research should extend the static, annual-aggregate impedance framework into a time-varying model by computing monthly or weekly OD impedance matrices. Complementary dimensions of network

This contribution has been peer-reviewed. The double-blind peer-review was conducted on the basis of the full paper.
https://doi.org/10.5194/isprs-annals-X-4-W8-2025-493-2026 | © Author(s) 2026. CC BY 4.0 License.

performance (such as passenger volumes, cargo flows, aircraft utilization rates, and airport slot constraints) should be incorporated into a multi-layer impedance matrix. Layer-specific weights or principal-component analysis can fuse these metrics with flight frequencies to yield richer depictions of accessibility, operational efficiency, and economic viability across core, regional, and peripheral segments. To inform contingency planning, the impedance matrix can be embedded in stochastic or agent-based models that simulate targeted perturbations (hub closures, route suspensions). Finally, applying the frequency-based OD impedance methodology to other national or continental networks will benchmark structural patterns, hub and spoke configurations and recovery trajectories. Cross country comparisons will clarify advancing both theoretical understanding and practical guidelines for airport network analysis.

## Acknowledgements

We sincerely thank the Iranian Airports and Air Navigation Company for sharing statistical data on flights from Iranian airports, separated by origin and destination, for this research.

## References

Ashwood, B. G., 2023. *Disruptions to the Cooperativity of DNA Base Pairing and Hybridization Probed With Temperature-Jump Infrared Spectroscopy* The University of Chicago.

Barceló, J., Montero, L., Bullejos, M., Linares, M., 2014. A practical proposal for using origin-destination matrices in the analysis, modeling and simulation for traffic management. 93rd TRB annual meeting compendium of papers,

Cascetta, E., 2013. *Transportation systems engineering: theory and methods* (Vol. 49). Springer Science & Business Media.

Ceha, R., Ohta, H., 1997. Prediction of future origin-destination matrix of air passengers by fratar and gravity models. *Computers & industrial engineering*, *33*(3-4), 845-848. https://doi.org/https://doi.org/10.1016/S0360-8352(97)00263-5

Cerqueira, S., Arsenio, E., Henriques, R., 2022. Inference of dynamic origin–destination matrices with trip and transfer status from individual smart card data. *European Transport Research Review*, *14*(1), 42. https://doi.org/https://doi.org/10.1186/s12544-022-00562-1

de Dios Ortúzar, J., Willumsen, L. G., 2024. *Modelling transport*. John wiley & sons.

Eghbali Mardekheh, M., Hamzeh, S., Neysani Samany, N., Argany, M. 2024. Assessing the groundwater vulnerability with DRASTIC and Fuzzy-AHP models and validating the results based on the nitrate concentration (Case study: Fumanat area, Guilan province). *Physical Geography Research*, *56*(4), 21-38. https://doi.org/https://doi.org/10.22059/jphgr.2024.365677.1007789

Fotheringham, A. S., 1983. A new set of spatial-interaction models: the theory of competing destinations. *Environment and Planning A: Economy and Space*, *15*(1), 15-36. https://doi.org/https://doi.org/10.1177/0308518X8301500103

Graham, A., Adler, N., Betancor, O., Bilotkach, V., Calderón, E. J., Martini, G., Niemeier, H.-M., Antunes, A. P., 2021. *Air transport and regional development methodologies*. Routledge.

Hake, I., & Karlsson, L., 2025. Integration and Evaluation of a Data-Driven Time-Sliced OD-Matrix in Traffic Models for Strategic Traffic Planning. In.

Kheiri, A., Karimipour, F., & Forghani, M., 2016. Intra-Urban Movement Patterns Estimation Based on Location Based Social Networking Data [Research]. *Journal of Geomatics Science and Technology*, *6*(1), 141-158. http://jgst.issgeac.ir/article-1-457-en.html. http://jgst.issgeac.ir/article-1-457-en.pdf

Kodanda, B., & Verma, A., 2011. Estimation of origin-destination air traffic flows from air transport movement data: an application to Indian domestic airport network system. 15th Annual Air Transport Research Society (ATRS 2011) World Conference, Sydney, Australia,

Rao, M., & Chaudhary, P., 2025. Flight Tracker-A Real Time Flight Tracking Application. *GRADIVA REVIEW*, *11*(5 2025), 189.

Šarić, J., Vidović, A., Štimac, I., & Mihetec, T., 2020. Specificity of the Franjo Tuđman airport position in the function of increasing regional competitiveness. Proceedings of the International Scientific Conference" The Science and Development of Transport"(ZIRP 2020),

Simini, F., González, M. C., Maritan, A., Barabási, A.-L., 2012. A universal model for mobility and migration patterns. *Nature*, *484*(7392), 96-100. https://doi.org/https://doi.org/10.1038/nature10856

WANG, C.-Y., & HU, S.-R., 2013. Estimation of time-dependent origin-destination matrices using the path flow proportion method. *Journal of the Eastern Asia Society for Transportation Studies*, *10*, 776-795. https://doi.org/https://doi.org/10.11175/easts.10.776

Wilson, A. G., 1971. A family of spatial interaction models, and associated developments. *Environment and Planning A*, *3*(1), 1-32. https://doi.org/https://doi.org/10.1068/a030001

Xiong, Z., Lian, D., Chen, E., Chen, G., & Cheng, X. (2023). Large-Scale OD Matrix Estimation with A Deep Learning Method. *arXiv preprint arXiv:2310.05753*. https://doi.org/https://doi.org/10.48550/arXiv.2310.05753

Zipf, G. K., 1946. The P 1 P 2/D hypothesis: on the intercity movement of persons. *American sociological review*, *11*(6), 677-686. https://doi.org/https://doi.org/10.2307/2087063

## Appendix

1. Interactive Radial Chart (Recorded Animation)
https://drive.google.com/file/d/1jYWGJAwnfA6GyZD4J7w94NkGgsc1UDG6/view?usp=sharing
2. Interactive Real Time Web GIS Flight Indicator (Recorded Animation)
https://drive.google.com/file/d/100sbTK_1zpbc3BCfeapMfIAoP5PAkwZX/view?usp=sharing
3. Iran Airports Graph
https://colab.research.google.com/drive/1pEpictlYYob-8qdh7xBwAygx6h5B3UdP?usp=sharing